Correspondence

DecaWave Ultra-Wideband Warm-Up Error Correction

In the field of indoor localization, ultra-wideband (UWB) technology is no longer dispensable. The market demands that the UWB hardware has to be cheap, precise, and accurate. These requirements lead to the popularity of the DecaWave UWB system. The great majority of the publications about this system deal with the correction of the signal power, hardware delay, or clock drift. It has traditionally been assumed that this error only appears at the beginning of the operation and is caused by the warm-up process of the crystal. In this article, we show that the warm-up error is influenced by the same error source as the signal power. To our knowledge, no scientific publication has explicitly examined the warm-up error before. This work aims to close this gap and, moreover, to present a solution, which does not require any external measuring equipment and only has to be carried out once. It is shown that the empirically obtained warm-up correction curve increases the accuracy for the two-way ranging significantly.

NOMENCLATURE

AltDS-TWR	Alternative double-sided TWR.
LOS	Line of sight.
PLL	Phase-locked loop.
RAM	Random-access memory.
SMD	Surface-mounted device.
TDOA	Time difference of arrival.
TOA	Time of arrival.
TOF	Time of flight.
TWR	Two-way ranging.
UWB	Ultra-wideband.

I. INTRODUCTION

Localization based on UWB technology is able to operate in indoor environments, where narrowband systems are mostly failing due to fading [1], [2]. In recent years, this technology has gained more attention and will play a significant role in the future [3]. This is mostly due to the declining price and size of the devices. One of the market

Manuscript received April 4, 2020; revised July 6, 2020, July 24, 2020, and July 29, 2020; released for publication July 30, 2020. Date of publication August 10, 2020; date of current version February 9, 2021.

DOI. No. 10.1109/TAES.2020.3015323

Refereeing of this contribution was handled by D. Qiu.

Authors' addresses: Juri Sidorenko is with the Fraunhofer Institute of Optronics, System Technologies and Image Exploitation, 76275 Ettlingen, Germany, and also with the Institute of Astronomical and Physical Geodesy, Technical University of Munich, 80333 Munich, Germany, E-mail: (juri.sidorenko@iosb.fraunhofer.de); Volker Schatz, Norbert Scherer-Negenborn, and Michael Arens are with the Fraunhofer Institute of Optronics, System Technologies and Image Exploitation, 76275 Ettlingen, Germany, E-mail: (volker.schatz@iosb.fraunhofer.de; norbert.scherer-negenborn@iosb.fraunhofer.de; michael.arens@iosb.fraunhofer.de); Urs Hugentobler is with the Institute of Astronomical and Physical Geodesy, Technical University of Munich, 80333 Munich, Germany, E-mail: (urs.hugentobler@tum.de). *(Corresponding author: Juri Sidorenko.)*

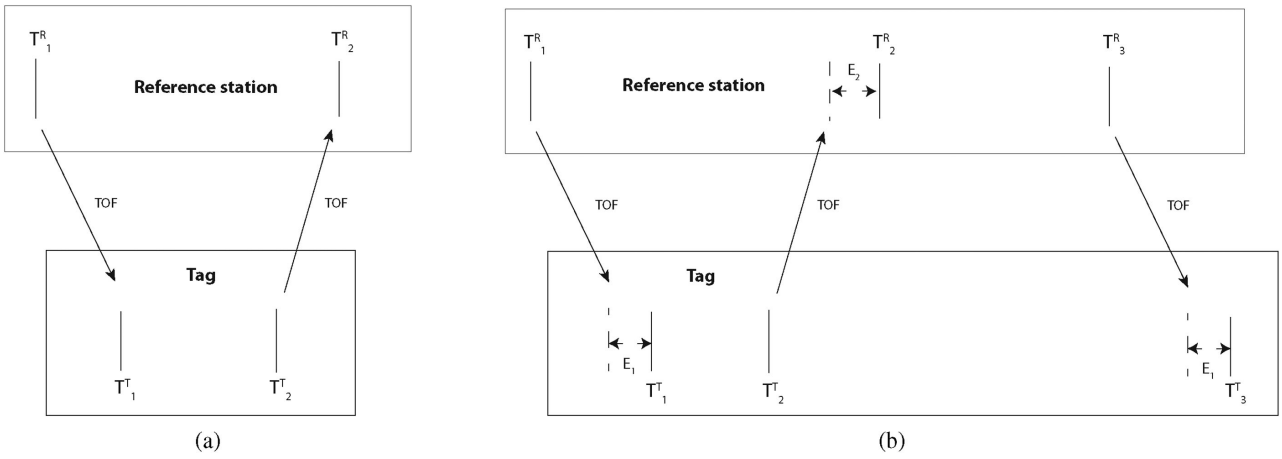

Fig. 1. Schematics of the TWR between the reference station and the tag. The timestamps of the reference station have the superscript index R and the tag index T. The shift of the timestamp caused by the signal power is labeled by E_1 and E_2. In (a), the TWR with two messages is presented, and in (b) the TWR with three messages is presented.

leaders is DecaWave Limited [4], whereby since 2019 the UWB device has been part of the new-generation Apple products [5] and will spark a revolution for augmented reality, smart home, mobile payments, keyless car entry, and indoor navigation [6]. The devices distributed by DecaWave are compliant with the IEEE802.15.4-2011 standard [7] and support six frequency bands with center frequencies from 3.5 to 6.5 GHz with data rates of up to 6.8 Mb/s. Depending on the selected center frequency, the bandwidth ranges from 500 to 1000 MHz. The sampling of the signal is performed by an internal 64-GHz chip with 15-ps event-timing precision (4.496 mm). Due to general regulations, the transmit power density is limited to −41.3 dBm/MHz. These regulations are due to the high bandwidth occupied by the UWB transceiver. The vast majority of all publications on the DecaWave system are focused on the correction of the hardware delay [8], the influence of the signal power on the timestamp [9], [10], and the clock drift [11]–[14]. Correcting these errors is very common for UWB systems [15]. Only few publications mention the warm-up error, which is attributed to the temperature fluctuation arising at power-up [16]–[18]. The influence of this error is reduced by waiting some time before the measurements are obtained [19] or by adapting the measurement error within the clock drift correction model [17], [20]. In practice, the accuracy obtained by the DecaWave device is about 10 cm for LOS applications [7]. In this article, we present a self-calibration method to obtain a correction curve for TWR and show how it is possible to obtain an accuracy better than 1 cm. The higher accuracy would allow further fields of application such as tomography, where signal power and flight time information can be used to determine the material between two transceivers.

The remainder of this article is structured as follows. The first part of this article deals with the TWR and how it is affected by the clock drift. Afterward come the experiments, which are used to gain new information about the source of the warm-up error. Finally, the conclusion is provided.

II. TWR PROTOCOL

The TWR protocol counts as a TOA measurement technique [21]. Its purpose is to provide distance measurements between two transceivers, even if they are not synchronized. In Fig. 1(a), the concept of TWR between two stations, the reference and the tag, is presented. The reference station initiates the ranging process by transmitting a message at the local time T_1^R. The tag receives the message at its local time T_1^T, and at the time T_2^T, it sends a response message back to the reference station. The TOF $\mathrm{TOF} = 0.5 \cdot (\Delta T_{1,2}^R - \Delta T_{1,2}^T)$ can be obtained by subtracting the response time $\Delta T_{1,2}^T = (T_2^T - T_1^T)$ from the transmitting and receiving time difference of the reference station $\Delta T_{1,2}^R = (T_2^R - T_1^R)$. Due to small imperfections, the frequencies of their clock crystals are not identical. In [14], a three-message-based clock drift correction protocol was presented, the so-called AltDS-TWR. This protocol has a small residual error, which only depends on the TOF. For the sake of completeness, it should be mentioned that an alternative protocol also exists with the same residual error [11]. However, this alternative protocol is strongly connected to the PLL, and in [22], we have shown that the PLL is affected by the signal power. In order to avoid cross-dependencies between the errors, we used the AltDS-TWR protocol. Fig. 1(b) illustrates the way this protocol works. The first steps are equivalent to Fig. 1(a), whereby the only difference is that the reference station transmits a third message at its local time T_3^R, which is also received by the tag at its local time T_3^T. Without a clock drift between the two stations, the time difference $\Delta T_{1,3}^R = (T_3^R - T_1^R)$ is equal to $\Delta T_{1,3}^T = (T_3^T - T_1^T)$. If this is not the case, it is possible to interpolate linearly the clock offset to correct the ranging time stamps. Another difference between Fig. 1(a) and (b) is the shift E_1 and E_2 of the timestamp caused by signal power. In [22], we have shown that it is possible to create automatically a correction curve between the received signal power and the timestamp shift. Previously, it was the state of the art to use a correction

curve based on the distance measurement and the ground truth distance [9]. The shift of the timestamp affects the timestamps T_1^T and T_3^T equally, under the assumption that the stations do not move during this message exchange of approximately 1 ms. The equal shift of both timestamps has the advantage that the signal power does not affect the clock drift correction. The hardware delay mainly depends on the temperature and can be estimated before the ranging [8], whereby this parameter is neglected for this article, due to the fact that the ambient temperature was almost constant during the experiments.

III. EXPERIMENTS

In the previous section, we have discussed the well-studied clock drift correction. In this section, it is time to focus on the often neglected warm-up error. At this point, we deviate from the classical structure and immediately come to the experiments. The reason for this is that the experiments form the core element of our assumptions about the source of the warm-up error. The following experiments were carried out with the Decawave EVK1000 and an update rate of 80 Hz. This board mainly comprises a DW1000 chip and an STM32 ARM processor.

The experiments are structured as follows.

1) The experiment presented in Section III-B examines whether there is a dependence between the distance and the warm-up error.
2) The experiment described in Section III-C examines whether the changing transmitter gain affects the warm-up error.
3) In the experiment described in Section III-D, the frequency difference is trimmed, to analyze the effects of the frequency difference on the received signal power and the warm-up error.
4) In the last experiment presented in Section III-E, the frequency difference as well as the transmitter gain are trimmed, to show how both parameters affect the warm-up error.

Section III-F summarizes the results and offers an explanation for the observations. This section does not appear before the experiments, because if the obtained dependencies are deterministic and measurable, it is possible to provide an empirical correction curve that can be generated by self-calibration, as shown in Section IV-B. This also applies to the case when not all observations can be theoretically explained.

A. Setup and Typical Distance Measurement

In Fig. 2, the experimental setup with two stations is presented. Unless otherwise stated, the stations have a distance of 1.5 m to each other. In the upcoming figures, the filtered values are presented, and unless otherwise stated, a moving average filter with a filter size of 500 measurements was used. The selected filter width is suitable to reduce the noise of the system without impairing the dynamics of the system too much. The distance measurements were

Fig. 2. Experimental setup with two stations mounted on a tripod.

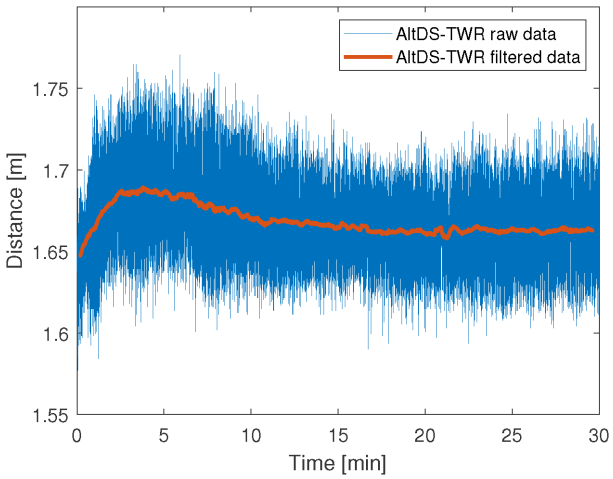

Fig. 3. Filtered typical distance measurement (in meters) over the time (in minutes) provided by the AltDS-TWR protocol.

all obtained with the AltDS-TWR protocol described in Section II. The signal power was measured at the reference station for the upcoming experiments. In Fig. 3, a typical curve of the distance measurements as a function of time is presented. Repeating the experiment with the same stations and same setup would lead to the same shape of the curve. In the Fig. 4, the distance measurement was repeated three times for two other stations. The filtered data show that the curve is deterministic under the same conditions, such as signal strength, pulse repetition rate, preamble length, and hardware structure. It can be observed that it takes up to 15 min before the curve reaches a constant value. The difference between the final value reached and the ground truth distance of 1.5 m is due to the hardware delay. This difference is irrelevant in this publication, due to the fact that it can be assumed to be constant. A possible explanation why the curve in Fig. 3 is not straight could be due to the change in the reference station frequency. The residual

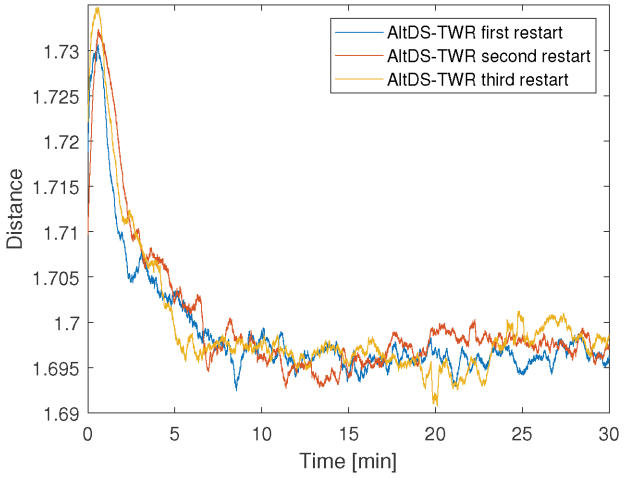

Fig. 4. Filtered typical distance measurement (in meters) over the time (in minutes) provided by the AltDS-TWR protocol with alternative stations. The range measurements were repeated three times after a pause of 10 min.

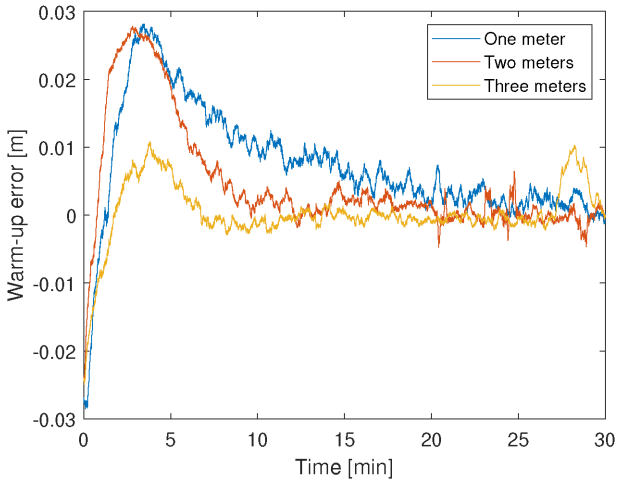

Fig. 5. Results of the first experiment with distance changes between the stations from 1 to 3 m. The curves represent the distance error over the time for different distances.

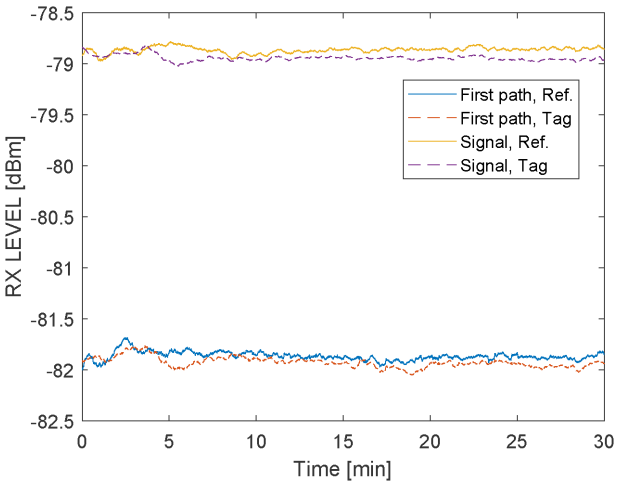

Fig. 6. Results of the first experiment with first path and total received signal power in [dBm] of the reference station (Ref.) and the tag. The dashed lines represent the received power measured at the tag station and the regular line at the reference station. The distance between the stations was 1.5 m.

error of the AltDS-TWR protocol depends on the TOF multiplied by the frequency change of the reference station. The DecaWave EVK1000 used is driven by an RSX-10 Rakon SMD crystal oscillator with a tolerance up to 50 parts per million (ppm) [23]. However, the TOF multiplied with the maximum change of the crystal oscillator offset is too small to cause an error of 3 cm. Therefore, it can be assumed that the source of this error is not the AltDS-TWR protocol. In [10], it is stated that the error at the beginning is due to the warm-up of the crystal oscillator after it is activated. This means that this error should not appear later on in the ranging process and is independent of the distance. This question justifies the first experiment shown in the next section.

B. First Experiment: Distance and Distance Error

In the first experiment, the distance between the reference station and the tag is changed stepwise from 1 m up to 3 m. Data are acquired for 30 min, and the last value in the sequence is subtracted from every distance measurement, because the focus is on the change over time. The subtracted distance measurements are labeled as distance errors for now. After every measurement, the device is unplugged from the power for 10 min to restore the initial condition. Fig. 5 shows the results of the first experiment. The blue curve is the distance error with a 1-m distance, the red line 2 m, and the yellow 3 m. It can be observed that the error at the beginning of the measurement depends on the distance. This contradicts the assumption that this error is simply due to the warm-up of the crystal oscillator. One explanation could be the influence of the signal power, due to the change over time. Fig. 6 shows the first path and total received signal power of the reference station and the tag. It cannot be observed that the measured first path and the signal power are affected by the crystal warm-up. The TOF is too short to cause this difference, especially because the error at 5 min is the same for 1 and 2 m. Therefore, the outcome is connected to the signal power.

C. Second Experiment: Transmitter Gain and Warm-Up Error

In this experiment, the distance between the reference station and the tag is kept constant at 1.5 m, where only the transmitted signal power is changed. The received signal power can be read from a register at the receiving station. The frequency difference was determined, as described in Section II. As in the previous experiment, the stations are unplugged from the power for 10 min after every experiment, and the last value is subtracted from every measurement. The frequency difference between the stations is provided by $(1 - \frac{\Delta T^T_{1,3}}{\Delta T^R_{1,3}})$ in ppm. The transmitter gain was reduced from 12 to 0 dB, with a step size of 3 dB. The transmitter gain

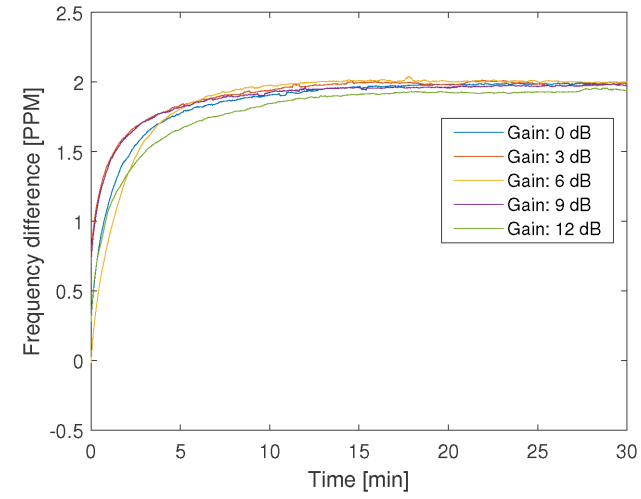

(a)

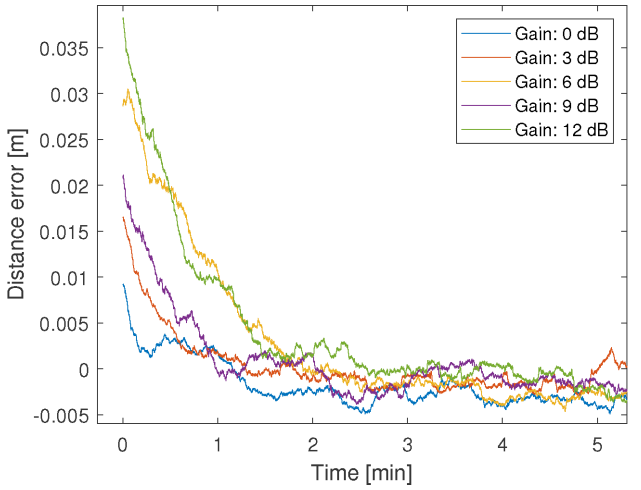

(b)

Fig. 7. Results of the second experiment. The curves represent the measurements of the (a) frequency difference and (b) distance error for different transmitter gains.

should not be confused with the actual transmitted signal power. The measured signal power differs from the actual signal power received with increasing signal strength [10]. The resulting frequency difference and the distance error are shown in Fig. 7. It can be observed that the signal strength has an influence on the frequency difference measured and the warm-up error. The question is whether this mutual dependence only arises in the first 15 min.

D. Third Experiment: Frequency Difference, Received Signal Power, and Distance Error

The DecaWave DW1000 IC allows centering the carrier frequency by adjusting the loading capacitance on the crystal oscillator [9]. The trimming is used to increase the receiver sensitivity by minimizing the frequency difference between the devices. In this experiment, the trimming is used to check whether the frequency difference affects the distance error. The ranging is performed with the transmitter gain of 12 dB. Fig. 8 shows that the trim value is changed stepwise until the final value is reached. In Fig. 8(a), it can be observed that the signal power increases the closer the frequency difference approaches zero, due to the increased sensitivity of the transceiver. The distance error, as shown in Fig. 8(b), is the highest at this point. It can be observed that the change over time is the higher, the closer the frequency difference is to zero.

E. Fourth Experiment: Frequency Difference, Changing Transmitter Gain, and Distance Error

The experiment in Section III-D is repeated with decreasing gain from 12 to 0 dB, with a step size of 3 dB. The signal gain is changed after the trim value reached its final value. This can be especially observed for the measurements with 9–12-dB signal gain at different times. In [22], we have shown how the correction curve between the received signal power and the timestamp shift can be obtained automatically. In Fig. 9(a), this curve is exemplarily presented. In Fig. 9(a), the distance measurements of this experiment are presented. It can be observed that this correction curve only applies for a certain frequency difference, which is not constant.

F. Interpretation of the Results

In Table I, the observations of the previous experiments are summarized. The first experiment states that the transmit power affects the frequency difference. The reason for this dependence is most likely the analog phase detectors of the PLL, in which the loop gain is a function of amplitude, affects the error signal, and, thus, also affects the pull-in time (total time taken by the PLL to lock). The results of the experiment in Section III-D state that the transmit power and frequency difference affect the received signal power. It is obvious that a higher transmitting power also causes a higher measured power received. This allows transferring more energy, and therefore, the measured signal power received is higher. The results of Sections III-D and III-E are the most interesting for ranging, because they affect the timestamp. The reason for the influence of the signal power and the frequency difference on the timestamp could be due to the leading edge detection (LDE) algorithm . This algorithm is a microcode loaded in the RAM of the DW1000 IC. It is executed on every frame reception to calculate the frame TOA [9]. It is not possible for the end user to change the code of this algorithm. After the digital sampling of the signal received, the LDE algorithm searches for the leading edge. The detected edge is ideally infinitely steep and higher than a certain threshold, as shown in case A of Fig. 10. In reality, the impulse is not infinitely steep and looks more like in case B. This leads to the threshold being passed earlier, and the set timestamp is not set at T_3 but at T_1. If the received signal power is now reduced, the new timestamp T_2 is closer to T_3 than T_1. With a smaller frequency difference between the transceivers, the PLL can better lock on to the received signal. With a higher signal spectrum or bandwidth, the impulse becomes sharper, as shown in case D of Fig. 10.

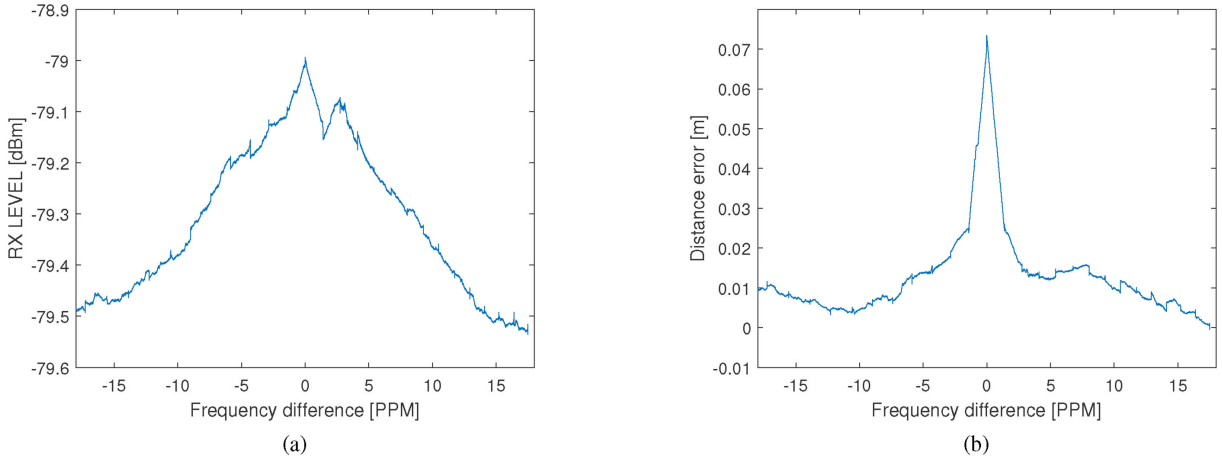

Fig. 8. Results of the third experiment with changing crystal trim over time. (a) Measured signal power. (b) Distance error.

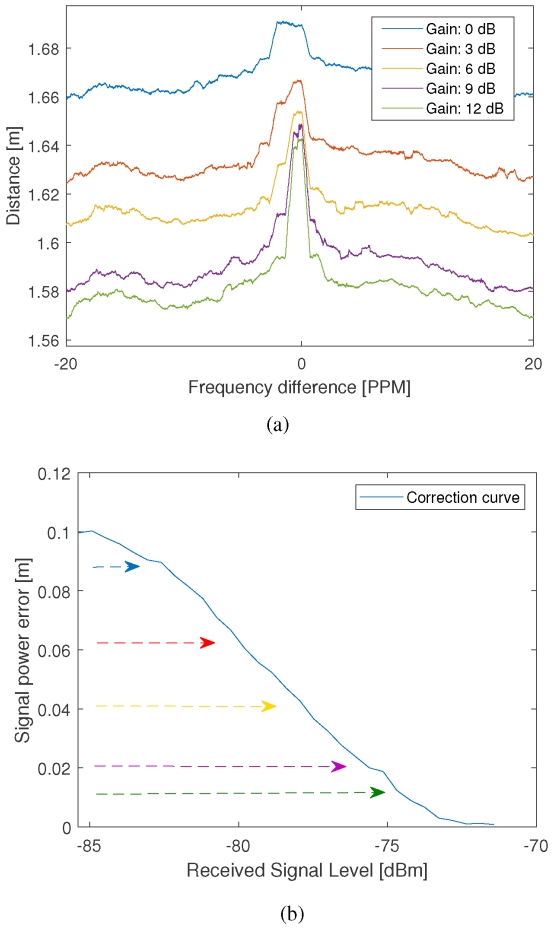

Fig. 9. Results of the fourth experiment. Relation between the signal power correction curve shown in (b) and the distance measurements shown in (a).

TABLE I
Observed Dependencies

Experiment-Sections	Cause	Effect
III-D	Transmit power and frequency difference	Received power
III-D and III-E	Transmit power and frequency difference	Timestamp

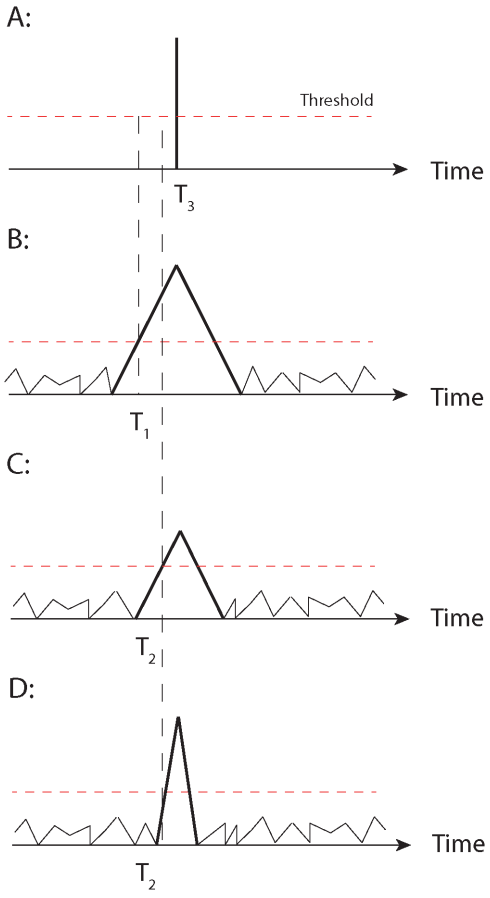

Fig. 10. LDE algorithm. A: Ideal case, B: High signal power, C: Low signal power, and D: High signal power and low frequency difference.

This also has an impact on the timestamp, which is now the same as in case C with a reduced signal power.

IV. CORRECTION

From the previous sections, we obtained the knowledge that the frequency difference has an influence on the measured signal power received. Furthermore, the received

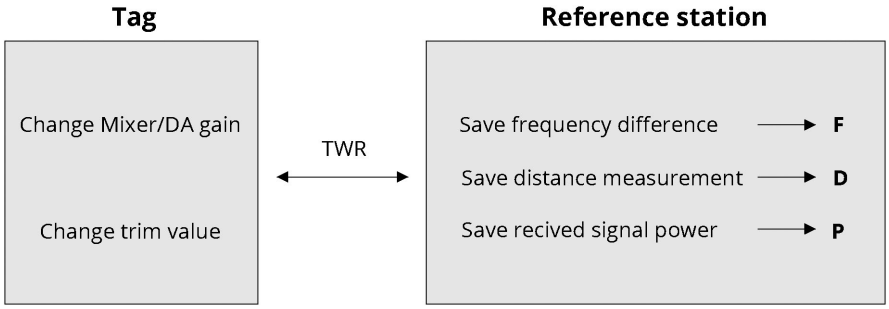

Fig. 11. Diagram for creating the correction values. The estimates of the frequency difference, the distance measurement, and the received signal power are stored in vectors F, D, and P.

signal power and the frequency difference lead to a shift of the timestamp. In this section, we show how the timestamp can be corrected.

The principle of the correction method is shown in Fig. 11. The distance between two stations is determined using TWR. The tag varies the Mixer/DA gain and the trim value. More detailed information on how this is done can be found in [9]. This variation can be realized with two loops. The reference station calculates the frequency difference, the distance, and the received signal strength. At this point, the calculated distance should be cleared of the influence of the clock drift. In Sections II and III-C, we show how the distance and the frequency difference can be determined, and source [9] explains in detail how the signal strength is obtained. During the ranging application, it is necessary that the calculated distance does not change over time, even if the frequency difference and the signal strength change. For this purpose, a reference value is determined in F and P; at this point, the correction value D is zero. With a regular distance measurement, the frequency difference, and signal strength are determined that come closest to a value in F and P. The corresponding value for D is subtracted from the distance measurement.

A. Dynamic Trim

The first presented approach is based on the implementation of a trimming routine during the ranging process at the reference station. The measured frequency offset between the two stations is used to trim the frequency with the aim of minimizing the difference. Fig. 12 shows the warm-up error during the dynamic trim. Due to two reasons, it was not possible to correct the warm-up error by dynamic trim: first, the PLLs of both devices tend to automatically reduce the frequency difference; and second, the step size of the trim is too high, at about 1.5 ppm. In the next section, it is shown that a step size of 1.5 ppm is too high to properly correct this error by dynamic trimming.

B. Correction Curves

In the fourth experiment from Section III-E, we have modified the signal power and trimmed the frequency difference to obtain the impact on the distance measurement.

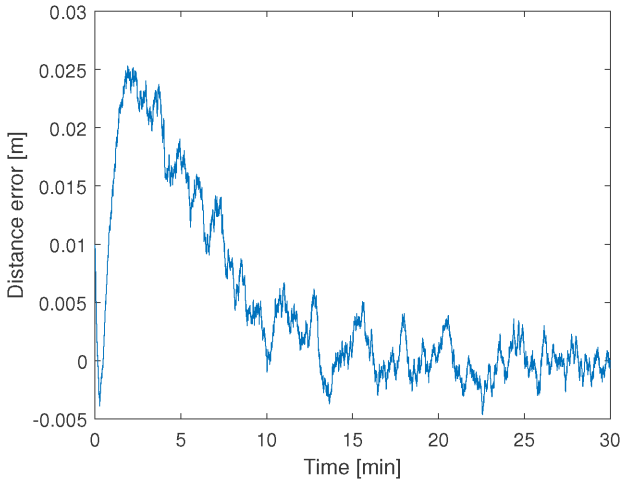

Fig. 12. Distance error during the dynamic trim.

To obtain data for use in a correction, the step size for the transmitter gain was reduced to 0.5 dB. Moreover, a moving average filter for smoothing the data is not used. The data are collected until the trim value or gain changes. This happens after 1000 measurements have been received. The mean of these 1000 measurements represents one data point. The results are shown in Fig. 13. A certain value of this plot can be used as a reference measurement. If the signal power or frequency difference changes, it is possible to correct the distance measured to maintain a constant value. The correction curve can be obtained automatically for two stations without additional measurement equipment. Unfortunately, the step size of the crystal trim is too high to sample the region close to zero frequency difference with sufficient accuracy, as shown in Fig. 14. The linear interpolation in this region is too inaccurate, and it is also possible that the value at zero is even higher. Alternatively, it is also possible to restart the device several times to obtain the dependence between the frequency difference and the distance measurement close to zero ppm. However, it is not practical, and the dependence between the frequency difference and the signal power is too complex to perform this kind of correction. It is better to sample the error for every combination of the signal power and frequency difference.

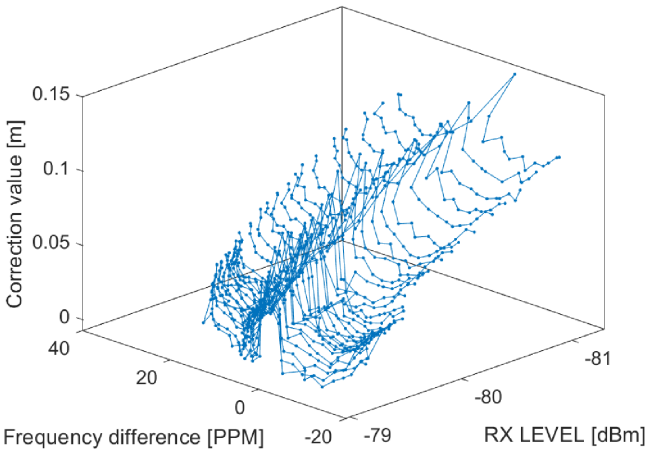

Fig. 13. Correction curve. Measured distance (in meters) with respect to the frequency difference (in ppm) and the signal power received (in dBm).

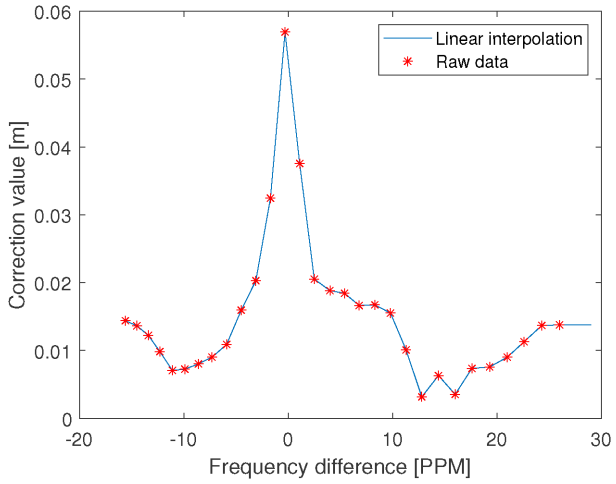

Fig. 14. Correction curve. Interpolation of the curve with the transmitted signal gain of 0 dB.

C. Validation of the Correction Curve

In the previous parts, it has been shown which parameter has an impact on the TWR and how a correction curve can be assembled. This section is dedicated to the validation of the correction curve. The measurement setup such as the station distance and filter size is equivalent to that of Section III.

The measurements take place at small and large frequency differences. The assumption is that due to the low sampling capability close to zero, the low-frequency-difference experiments become less accurate.

1) *Small Frequency Difference:* In the first test case, we do not use frequency trimming to reduce the frequency difference. Only the transmitter gain between both stations has been changed in this experiment. During the first 30 min, the gain was at 6 dB, while in the following, the gain was reduced to 3 and 0 dB, before it increased again to 9 and 12 dB. Between the power changes, the gain was set back to the initial value of 6 dB. After the first 30 min, every gain was measured for 5 min.

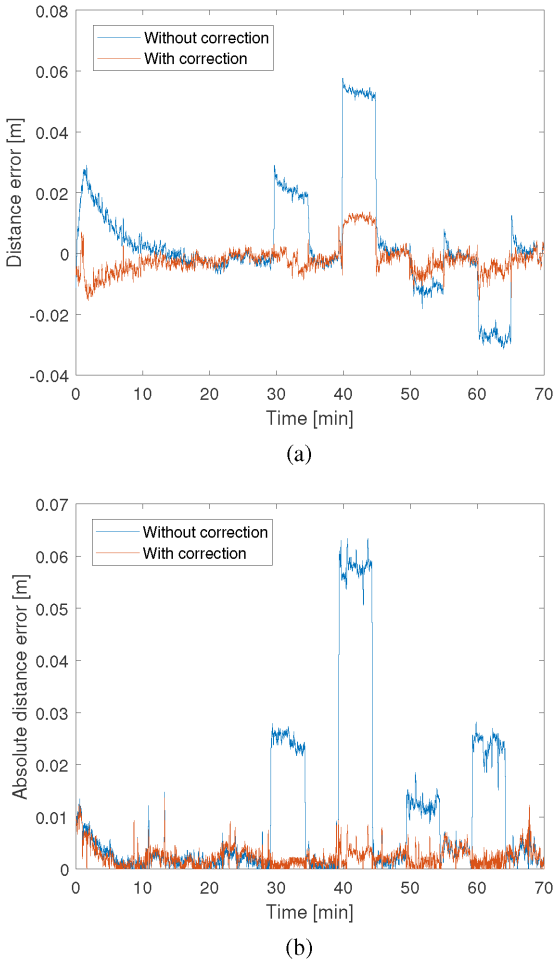

Fig. 15. Validation of the correction curve with (a) small and (b) large frequency difference.

TABLE II
Absolute Mean and Maximum Value of the Distance Error With Small Frequency Differences (SF) and Large Frequency Differences (LF)

	Mean [m]	Max [m]
SF without correction:	0.0108	0.0577
SF with correction:	0.0039	0.0155
LF without correction:	0.0103	0.0634
LF with correction:	0.0023	0.0137

The frequency difference and the received signal power have been used to find the corresponding correction values in the correction curve. In Fig. 15(a), the results of the TWR with and without correction are presented. It can be observed that the corrected values perform much better compared with the results without the correction. In particular, the distance error at the beginning is reduced by one-third. In some regions, such as between 40 and 45 min, the correction was not perfect. The reason is most likely that the frequency difference is very close to zero. In this area, it is not possible to obtain good correction values, due to the high step size of 1.5 ppm. Table II summarizes the mean of the absolute value and the maximum peak of the absolute value. The corrected values have a three times smaller error compared with the uncorrected values.

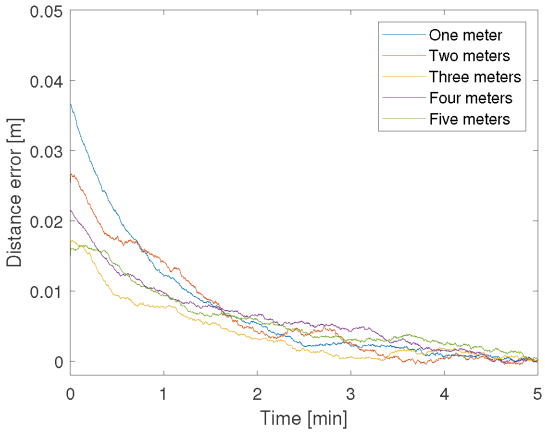

(a)

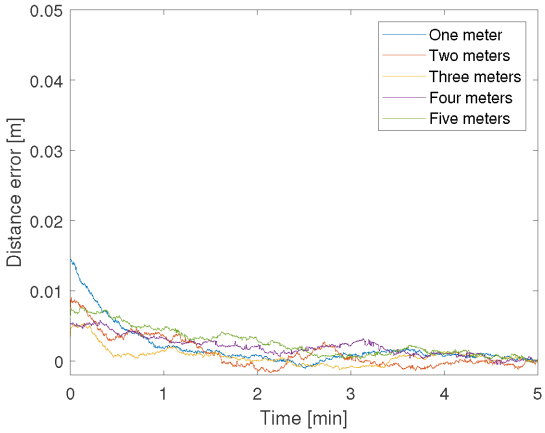

(b)

Fig. 16. Validation of the correction curve with small frequency difference for other stations and different distances. Distance error (a) without using the correction curve and (b) with using the correction curve.

To validate the results, we repeated this experiment for other stations with an alternative correction curve. It was not the signal strength that was changed, but the distance of the stations. After each change of position, the stations were restarted to initiate a warm-up phase. Fig. 16(a) shows the distance error of the uncorrected stations, while Fig. 16(b) shows the distance error of the corrected stations. Without the warm-up, the solution with changing distances is equivalent to the one presented in [22]. It can be clearly seen that the corrected values have a significantly smaller distance error than the uncorrected ones.

2) *Large Frequency Difference:* The setup of the second test case is equivalent to the previous test case. The only difference is that the system is trimmed from the beginning on, to obtain a higher offset. Further away from the frequency difference zero, we expect a smaller rate of change in the distance error. This should also decrease the uncorrected warm-up error. As observed in Fig. 14, the change of the error curve with respect to the input parameters is smaller. In Fig. 15(b), it can be seen that the distance error is smaller at the beginning, as expected. Moreover, the remaining error of the corrected curve is smaller compared with the first test case, especially between 40 and 45 min. The absolute mean and maximum distance errors are shown in Table II. Large frequency difference is great for applications where accurate measurements are required. In addition, small differences have a much smaller influence on the measurement. With dynamic trimming, it is possible to have a fixed frequency difference. This means that only the signal strength is required for the correction. The correction curves are no longer created via TWR but for each station individually. Therefore, they are also suitable for TDOA applications. More information on this topic can be found in [22].

V. CONCLUSION

In this article, we performed different practical experiments to identify the influence of the signal power and the frequency difference on the timestamp shift. It was shown that the error, known as the warm-up error, is strongly connected to the frequency difference between the devices. We showed that the warm-up error has the strongest impact at the beginning, but also appears later on in the ranging process. We presented a method that automatically creates a correction curve that can be used as a lookup table. This method can be used for any DecaWave chip-based station to correct TWR measurements. After the clock drift correction, the DecaWave DW1000 device has an accuracy of 10 cm for the TWR. If the impact of the signal power and the frequency difference is properly corrected, it is possible to obtain an accuracy smaller than 1 cm. The higher accuracy allows us to use this system in other technology fields such as tomography, with the aim of detecting the time delay caused by a penetrated material or the material itself. This would not be possible if the TOF measurements depended on the signal strength or frequency difference between the devices.

In order to accomplish this task, we presented a self-calibration solution that does not require additional measurement equipment or any change of the hardware. The correction lookup table can be created and saved independently on the devices. In the later course, this table can then be used for the correction of the distance measurements. Alternatively, it is also possible to change the hardware to reduce the step size for the clock frequency trim by additional capacitors. The dynamic trim with a smaller step size allows obtaining the correction curve for every station individually. At this point, the correction curve can be used for TOA as well as TDOA measurement techniques. In future work, the effect of temperature and voltage on frequency difference will be studied in more detail.

ACKNOWLEDGMENT

The authors would like to thank Dr. D. Bulatov from the Fraunhofer Institute of Optronics, System Technologies and Image Exploitation and two anonymous reviewers for reading this manuscript and providing ideas for its improvement.

JURI SIDORENKO

VOLKER SCHATZ

NORBERT SCHERER-NEGENBORN

MICHAEL ARENS

Fraunhofer Institute of Optronics, System Technologies and Image Exploitation Ettlingen, Germany

URS HUGENTOBLER

Technical University of Munich, Munich, Germany

REFERENCES

[1] J. F. M. Gerrits, J. R. Farserotu, and J. R. Long
Multipath behavior of FM-UWB signals
In *Proc. IEEE Int. Conf. Ultra-Wideband*, Sep. 2007, pp. 162–167.

[2] R. A. Saeed, S. Khatun, B. M. Ali, and M. A. Khazani
Ultra-wideband (UWB) geolocation in NLOS multipath fading environments
In *Proc. 13th IEEE Int. Conf. Netw./IEEE 7th Malaysia Int. Conf. Commun.*, Nov. 2005, pp. 6.

[3] D. Dardari, N. Decarli, A. Guerra, and F. Guidi
The future of ultrawideband localization in RFID
In *Proc. IEEE Int. Conf. RFID*, May 2016, pp. 1–7.

[4] A. R. Jiménez Ruiz and F. Seco Granja
Comparing Ubisense, BeSpoon, and DecaWave UWB location systems: Indoor performance analysis
IEEE Trans. Instrum. Meas., vol. 66, no. 8, pp. 2106–2117, Aug. 2017.

[5] *Online Article*. Accessed: Oct. 9, 2019. [Online]. Available: https://sixcolors.com/post/2019/09/the-u1-chip-in-the-iphone-11-is-the-beginning-of-an-ultra-wideband-revolution

[6] *DecaWave Markets*. Accessed: Oct. 9, 2019. [Online]. Available: https://www.decawave.com/markets-applications/

[7] M. Haluza and J. Vesely
Analysis of signals from the DecaWave TREK1000 wideband positioning system using AKRS system
In *Proc. Int. Conf. Mil. Technol.*, Jun. 2017, pp. 424–429.

[8] *DecaWave APS014 Application Note: Antenna Delay Calibration DW1000-Based Products and Systems*, Version 1.2. Accessed: Oct. 9, 2019. [Online]. Available: https://www.decawave.com

[9] *DW1000 User Manual*, Version 2.15. Accessed: Oct. 9, 2019. [Online]. Available: https://www.decawave.com

[10] *DecaWave APS011 Application Note: Sources of Error in TWR*, Version 1.0. Accessed: Oct. 9, 2019. [Online]. Available: https://www.decawave.com

[11] I. Dotlic, A. Connell, and M. McLaughlin
Ranging methods utilizing carrier frequency offset estimation
In *Proc. 15th Workshop Position., Navigat. Commun.*, Oct. 2018, pp. 1–6.

[12] R. Hach
Symmetric double sided two-way ranging
Jun. 2005. [Online]. Available: http://www.ieee802.org/15/pub/TG4a.html

[13] Y. Jiang and V. C. M. Leung
An asymmetric double sided two-way ranging for crystal offset
In *Proc. Int. Symp. Signals, Syst. Electron.*, Jul. 2007, pp. 525–528.

[14] D. Neirynck, E. Luk, and M. McLaughlin
An alternative double-sided two-way ranging method
In *Proc. 13th Workshop Position., Navigat. Commun.*, Oct. 2016, pp. 1–4.

[15] J. Sidorenko, V. Schatz, N. Scherer-Negenborn, M. Arens, and U. Hugentobler
Error corrections for ultra-wideband ranging
IEEE Trans. Instrum. Meas., to be published, doi: 10.1109/TIM.2020.2996706.

[16] R. Zandian and U. Witkowski
Robot self-localization in ultra-wideband large scale multi-node setups
In *Proc. 14th Workshop Position., Navigat. Commun.*, 2017, pp. 1–6.

[17] V. Navrátil, J. Krška, F. Vejražka, and V. Koreček
Chained wireless synchronization algorithm for UWB-TDOA positioning
In *Proc. IEEE/ION Position, Location, Navigat. Symp.*, 2018, pp. 149–157.

[18] R. Zandian and U. Witkowski
Implementation challenges of synchronisation of UWB nodes in TDoA structures
In *Proc. Int. Conf. Indoor Position. Indoor Navigat.*, 2018, pp. 1–8.

[19] J. Cano, S. Chidami, and J. L. Ny
A Kalman filter-based algorithm for simultaneous time synchronization and localization in UWB networks
In *Proc. Int. Conf. Robot. Automat.*, 2019, pp. 1431–1437.

[20] A. Ledergerber, M. Hamer, and R. D'Andrea
A robot self-localization system using one-way ultra-wideband communication
In *Proc. IEEE/RSJ Int. Conf. Intell. Robots Syst.*, 2015, pp. 3131–3137.

[21] D. L. Adamy
EW 102: A Second Course in Electronic Warfare. Boston, MA, USA: Artech House, Jul. 2004.

[22] J. Sidorenko, V. Schatz, M. Arens, N. Scherer-Negenborn, and U. Hugentobler
DecaWave UWB clock drift correction and power self-calibration
Sensors, vol. 19, Jul. 2019, Art. no. 2942.

[23] *Product Manual RSX-10*. Accessed: Oct. 9, 2019. [Online]. Available: http://www.rakon.com